Original Article
Synthesis and pre-clinical evaluation of an ^{18}F-labeled single-chain antibody fragment for PET imaging of epithelial ovarian cancer

Sai Kiran Sharma[1,2], Melinda Wuest[1], Jenilee D Way[1], Vincent R Bouvet[1], Monica Wang[1], Frank R Wuest[1,2]

[1]Department of Oncology, Cross Cancer Institute, University of Alberta, Edmonton, AB, T6G 1Z2, Canada; [2]Faculty of Pharmacy and Pharmaceutical Sciences, Katz Centre for Pharmacy and Health Research, University of Alberta, Edmonton, AB, T6G 2E1, Canada

Abstract: Anti-CA125 antibodies have been used in immunoassays to quantify levels of shed antigen in the serum of patients who are under surveillance for epithelial ovarian cancer (EOC). However, there is currently no molecular imaging probe in the clinic for the assessment of CA125 expression *in vivo*. The present study describes the development of an ^{18}F-labeled single-chain variable fragment (scFv) for PET imaging of CA125 in preclinical EOC models. Anti-CA125 scFv was derived from MAb-B43.13 by recombinant expression of the fragment in *E.coli.* Fragment scFv-B43.13 was purified via immobilized metal affinity chromatography and characterized for antigen binding via immuno-staining and flow cytometry. Prosthetic group *N*-succinimidyl 4-[^{18}F]fluorobenzoate ([^{18}F]SFB) was used for radiolabeling of scFv-B43.13. Preclinical ovarian cancer models were developed based on ovarian cancer cell lines OVCAR3 (CA125-positive) and SKOV3 (CA125-negative) in NIH-III mice. The radiopharmacological profile of ^{18}F-labeled scFv-B43.13 ([^{18}F]FBz-scFv-B43.13) was studied with PET. [^{18}F]FBz-scFv-B43.13 was prepared in radiochemical yields of 3.7 ± 1.8% (n = 5) at an effective specific activity of 3.88 ± 0.76 GBq/μmol (n = 5). The radiotracer demonstrated selective uptake in CA125-positive OVCAR3 cells and virtually no uptake in CA125-negative SKOV3 cells. Standardized uptake values (SUV) of radioactivity uptake in OVCAR3 tumors was 0.5 (n = 3) and 0.3 (n = 2) in SKOV3 tumors after 60 min post injection (p.i.).

Keywords: CA125, positron emission tomography, epithelial ovarian cancer, fluorine-18

Introduction

Rapid advances in recombinant DNA technology combined with an expanding scope of using a variety of radionulcides for positron emission tomography (PET) have transformed PET into a highly versatile technique that employs engineered antibody formats for molecular imaging of cancer [1, 2]. Single-chain antibody fragment (scFv) combining the variable heavy and light chain domains of an immunoglobulin molecule are capable of binding with target antigens including tumor biomarkers [3]. Single-chain antibody fragments also serve as popular formats for the engineering of antibodies. Typically one-fifth the size (~28 kDa) of a full-length antibody (~150 kDa), scFv(s) offer some theoretically compelling advantages including better tumor penetration combined with rapid system-ic clearance that can yield high tumor-to-background ratios at early time points. Their amenability to genetic engineering can facilitate many advantages including - a) site-specific labeling; b) an increase in the avidity via multimerization; and c) enhancement of the binding affinity via site-directed mutagenesis. Further, the absence of an immunoglobulin's Fc portion and its downstream modulation of the immune system renders it as a relatively non-immunogenic targeting vector *in vivo* [4]. While the selection of a specific targeting molecule constitutes one arm of an immuno-PET strategy, the other involves the selection of an appropriate radionuclide that partners in the development of a suitable radiotracer. In this context, ideal image contrast and information may be obtained as a result of an ideal match between the biological half-life of the targeting vector and the physical half-life

of the radionuclide [5]. Thus, it is a logical choice that antibody fragments such as scFv (28-30 KDa) and diabodies (56-60 KDa), which have molecular weights below the cut-off for renal clearance and demonstrate relatively short biological half-lives (0.5-7 h) should be radiolabeled with positron-emitting radionuclides such as fluorine-18 (^{18}F) and/or gallium-68 (^{68}Ga), which have physical half-lives of 109.8 min and 68 min respectively [6].

Availability of many on-site biomedical cyclotrons worldwide and the ease of production have contributed to an almost unlimited access of ^{18}F and its routine use for clinical [^{18}F]FDG-PET imaging. Most clinical PET scanners are calibrated for using ^{18}F. Other advantages associated with using ^{18}F as the radionuclide of choice for PET imaging include a) the 97% positron emission yield, b) the low energy of the emitted positrons, and c) the lack of interfering radiations that results in high-resolution images. All these factors indicate the potential and advantages of ^{18}F-labeled radiotracers for clinical translation.

The ability to accomplish same-day imaging in patients with ^{18}F represents the ideal situation in clinical PET imaging. In the context of immuno-PET imaging, this can be achieved through the development of radiotracers that combine the short biological half-lives of antibody fragments with short-lived PET-radionuclides. Conversely, the use of full-length antibody radioimmuno-conjugates requires radiolabeling with longer-lived isotopes that may pose a higher radioactive burden to patients throughout the course of the radioimmunoconjugate's specific accumulation in tumors and its concomitant clearance from the systemic circulation over a period of days to weeks.

Epithelial ovarian cancer (EOC) is the most lethal gynecologic malignancy and is characterized by the overexpression of cancer antigen 125 (CA125) - a high molecular weight mucinous glycoprotein [7]. Expression of CA125 has also been reported in breast cancer, mesothelioma, leiomyoma, and some benign conditions such as endometriosis, ovulatory cycles, congestive heart failure and liver disease [8]. At present, CA125 expression is assayed in serum samples from patients who present in the clinic with pelvic masses suspected for ovarian cancer [9]. Among the antibodies used in such

immunoassays, MAb-B43.13 - a CA125-targeted murine monoclonal antibody has been used for the immunotherapy of EOC [10-12]. Besides [^{18}F]FDG - a metabolic radiotracer used for the functional imaging of several cancers [13], there is currently no targeted PET radiotracer available for same-day non-invasive imaging of ovarian cancer.

Here, we synthesized a CA125-targeted scFv and developed a molecular imaging probe to achieve same-day imaging of EOC via immuno-PET. The anti-CA125 scFv was derived from MAb-B43.13 via recombinant expression and radiolabeled with ^{18}F ($t_{1/2}$ 109.8 min) using N-succinimidyl-4[^{18}F]fluorobenzoate ([^{18}F]SFB) as a prosthetic group. The ^{18}F-labeled scFv-[^{18}F]FBz-scFv-B43.13 was analyzed in vitro and in vivo using CA125-positive OVCAR3 cells and CA125-negative SKOV3 cells in subcutaneous xenograft mouse models of EOC. A radiofluorinated version of the complete antibody - [^{18}F]FBz-MAb-B43.13 - was used as a positive control to evaluate the immunoreactivity of the antibody fragment.

Materials and methods

Production of scFv-B43.13 and MAb-B43.13

The scFv-B43.13 was produced as described previously [14]. Briefly, genes encoding the heavy (V_H) and light chains (V_L) of the scFv were cloned in a pET-22b(+) plasmid vector (Novagen, 69744) for recombinant expression in E.coli Rosetta 2(DE3) (Novagen, 71400). Single transformant colonies were grown in 2 litre bacterial cultures and induced with 0.8 mM Isopropyl-β-D-thiogalactopyranoside (IPTG) (Fisher Scientific, BP1755-10). The cells were cultured for 16 h at 26°C prior to harvesting the biomass by centrifugation at 7000 rpm for 30 minutes. The cell pellet was treated with BugBuster Master Mix (Novagen, 71456) to extract the soluble protein from the bacterial periplasm. The scFv-B43.13 was purified via immobilized metal affinity chromatography using TALON® Superflow resin (Clontech, 63-5506). 1 mL elution fractions were collected and analyzed by 12% SDS-PAGE and immunoblotted for the C-terminal hexa-histidine tag using 6X His MAb-HRP conjugate (Clontech, 631210). The eluted fractions that had high concentrations of the purified scFv were pooled together and dialyzed in phosphate buffered

A

B
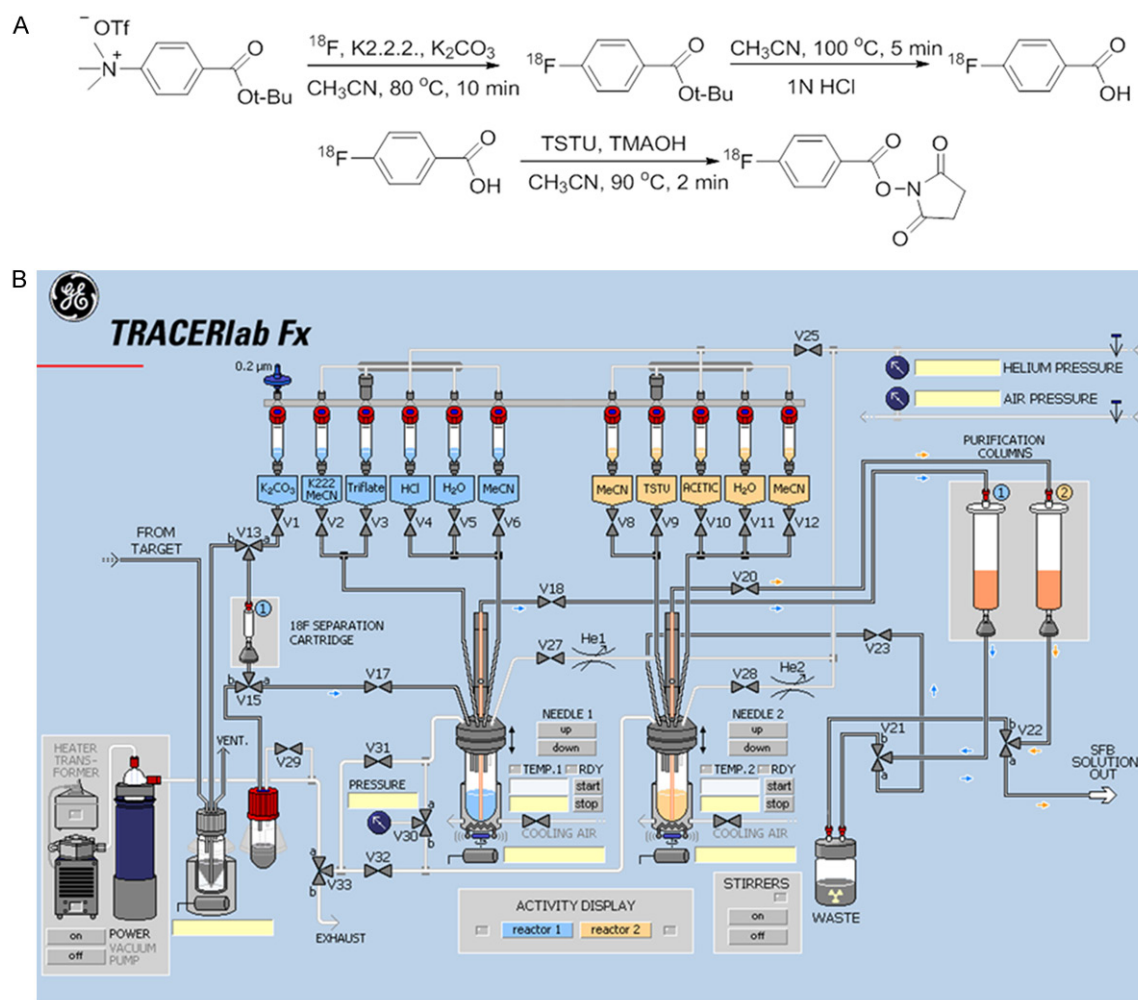
Figure 1. Synthesis of *N*-succinimidyl-4-[^{18}F]fluorobenzoate ([^{18}F]SFB). A. Chemical reaction scheme for the synthesis of [^{18}F]SFB; B. Layout of the TRACERlab automated synthesis unit (GE) used for the synthesis of [^{18}F]SFB.

saline (pH 7.4) to remove the excess imidazole and concentrated via centrifugation using Amicon Ultra-15, 10K MWCO filters (EMD Millipore, UFC901024). The monoclonal antibody (MAb-B43.13) was purified from the hybridoma (kindly provided by Quest PharmaTech Inc. Canada) cell culture supernatant via protein G affinity (Sigma, P-7700) on a BioLogic DuoFlow™ chromatography system (Bio-Rad, 760-0135). Final concentrations of the purified scFv and MAb were quantified using a Pierce™ BCA protein assay kit (Thermo Scientific, 23227).

Cell lines and culture conditions

Ovarian cancer cells-OVCAR3 (ATCC® HTB-161™) that overexpress CA125, and SKOV3 (ATCC® HTB-77™) that do not express CA125 were used for *in vitro* functional characteriza-

tion studies. Cells were cultured in DMEM-F12 medium supplemented with 10% v/v fetal bovine serum (Life Technologies, 12483-020), 50 IU/mL penicillin, 50 µg/mL streptomycin (Life Technologies, 15140-122).

OVCAR3 cells were additionally supplemented with 7 µg/mL recombinant human insulin (SAFC Biosciences, 91077C). Cells were cultured using sterile techniques and grown in a 37°C incubator providing humidified atmosphere of 5% CO_2 in air.

Functional characterization of scFv-B43.13

Fluorescent labeling of 2 mg MAb-B43.13 (4 mg/mL) and scFv (2 mg/mL) was carried out using the Pierce FITC antibody labeling kit (Thermo Scientific, 53027).

Flow cytometry: 1.5×10^6 OVCAR3 cells were harvested by trypsinization and rinsed twice with FACS buffer (PBS with 0.5% heat inactivated FBS, 2 mM EDTA, 0.05% sodium azide) before resuspending the cells by gentle tapping in ~100 µL of this buffer. 10 µg of FITC-MAb-B43.13, FITC-scFv-B43.13, unlabeled scFv-B43.13, and a hexa-histidine tagged anti-RANK binding scFv (isotype control) were incubated with the OVCAR3 cells for 30 min at room temperature. Cells were rinsed thrice with FACS buffer and samples that were previously incubated with unlabeled scFv were then incubated for 30 min with 2.4 µg of Penta·His Alexa Fluor 488 conjugate (Life Technologies, A-11001). OVCAR3 cells were rinsed thrice with FACS buffer and analyzed by flow cytometry on a BD FACS Calibur. 10,000 events were gated for analysis per sample. Negative controls included unstained OVCAR3 cells and cells incubated with Penta·His Alexa fluor 488-conjugated antibody alone.

Immunofluorescence: OVCAR3 and SKOV3 cells were plated onto glass coverslips in 35-mm tissue culture dishes (100,000 cells/2 mL medium/dish) and incubated at 37°C for 48 h. Cells were rinsed with PBS and fixed in methanol for 30 min at -20°C. The fixed cells were incubated in 5% non-fat dry milk (Carnation) in PBS and immunostained separately for 1 h with 1 mg/mL (1:250 dilution) of FITC-MAb-B43.13 and FITC-scFv-B43.13, unlabeled scFv-B43.13, anti-RANK scFv (isotype control). Penta·His Alexa Fluor 488 conjugate (2 mg/mL; 1:500 diluton) in PBS containing 5% non-fat dry milk was used as a secondary antibody to probe for unlabeled scFv-B43.13 and the anti-RANK scFv. Appropriate blank and control samples were included in the experiments. All antibody incubations were followed by three rinses with PBST for 10 min each. Coverslips were mounted on microscopy slides (Fisherbrand) using Mowiol® mounting medium (Calbiochem, 475-904) supplemented with DAPI (50 µg/mL). Immunofluorescence was observed through a Zeiss Plan Apochromat 40X/1.3 oil DIC M27 lens on a confocal laser scanning microscope (Zeiss LSM 710). The images were analyzed using Zen 2011 software and processed using Adobe Photoshop CS6.

Synthesis of [18F]SFB

[18F]SFB was synthesized on an automated synthesis unit as per a previously reported method

[15]. Non-carrier added [18F]fluoride was produced via an $^{18}O(p,n)^{18}F$ nuclear reaction from [18O]H₂O (Rotem Industries Ltd, Hyox oxygen-18 enriched water, min. 98%) on an ACSI TR19/9 Cyclotron (Advanced Cyclotron Systems Inc., Richmond, Canada). Radiosynthesis of *N*-succinimidyl-4-[18F]fluorobenzoate was performed on a GE TRACERlab™ FX (General Electric Company, Fairfield, Connecticut, United States). The ASU was modified for the program and hardware as shown (**Figure 1**).

The synthesis was initiated by the elution of resin-bound cyclotron-produced [18F]fluoride from a Waters Sep-Pak®light QMA anion exchange column into the Reactor 1 (R1) of the GE TRACERlab™ FX using a solution of 86% $K_{2.2.2}/K_2CO_3$ (1.5 mL). [18F]Fluoride was dried azeotropically (V2, CH_3CN, 1.5 mL) under vacuum and a steady stream of nitrogen at 50°C and 95°C. *Tert.*-butyl 4-*N,N,N*-trimethylammoniumbenzoate triflate (V3) in CH_3CN (1 mL) was added to the dried [18F]fluoride, and reacted at 80°C for 10 minutes. Once the reaction was completed and cooled, 1 N HCl (V4, 1.0 mL) was added and allowed to react for an additional 5 minutes at 100°C. After de-protection, the mixture was diluted with water (V5, 12 mL) and passed through a Macherey-Nagel Chromabond® HR-P M (330 mg, Purification Column 1). 4-[18F]fluorobenzoic acid ([18F]FB) was eluted off in CH_3CN (V6, 3 mL) into Reactor 2 (R2), which pre-contained 25 wt% tetramethylammonium hydroxide in methanol (35 µL) in CH_3CN (0.5 mL). [18F]FB was additionally dried azeotropically (V8, CH_3CN, 1.5 mL) under vacuum and a steady stream of nitrogen at 50°C and 95°C to reduce the volume from 3 mL to 0.5 mL. To the volume reduced [18F]FB, N,N,N,N-Tetramethyl-O-(N-succinimidyl) uronium tetrafluoroborate (V9, 40 mg) in CH_3CN (1 mL) was added and reacted at 90°C for 2 minutes. Once completed, the mixture was diluted with 5% acetic acid (V10, 12 mL) and passed through a Macherey-Nagel Chromabond® HR-P M (330 mg, purification column 2). The purification column 2 was additionally washed with water (V11, 10 mL) and the final product was eluted in CH_3CN (4 mL) through a Waters SepPak Silica Plus column into a 10 mL sealed collection vial with a vent needle.

SFB labeling of scFv-B43.13

The [18F]SFB was purified by HPLC on a semi-preparative Luna C18 column (Phenomenex,

100 Å, 10 µm, 250 × 10 mm) using a gradient elution of acetonitrile:water at a flow rate of 3 mL/min monitored under UV at 254 nm and a dedicated radioactivity flow monitor (HERM) detection of the radioactivity trace. 1 Giga-bequerel (GBq) of the ASU-synthesized [18F]SFB was injected into the semi-preparative HPLC column and the purification was initiated with an acetonitrile:water elution gradient of 15:85 reaching 50:50 (v/v) in 12 min. This was allowed to stay at 50/50 (v/v) for 1 minute before resuming a 6 minute elution gradient from 50:50 to 70:30 (v/v), which was used as the final eluent ratio of acetonitrile:water over the last 11 minutes of a 30 min HPLC run. [18F]SFB corresponding to the area under the curve from the HPLC radiotrace was collected in a 50 ml pear shaped flask (Ace glass, 9477-27). The HPLC-purified [18F]SFB was concentrated to dryness on a rotary evaporator set at 35°C. 100 µg of anti-CA125 scFv (2 mg/mL) in 50 mM borate buffer pH 8.3 was added to the dried [18F]SFB and mixed well by adding an additional 450 µL of borate buffer to dissolve the two reactants prior to transferring the reaction mixture into a Protein LoBind 1.5 mL tube (Eppendorf, 13698794). The reaction was allowed to proceed in a thermal shaker set at 30°C, 550 rpm for 45 minutes. [18F]-labeled scFv was further purified by passing the reaction mixture through an Econo-Pac® 10DG desalting column (Bio-Rad, 732-2010) pre-equilibrated with 0.9% saline (Becton Dickinson, 306572), which was also used as the eluent for purification of the 18F-labeled scFv-B43.13. 350 µL elution fractions were collected from the desalting column and the associated radioactivity was measured on an Atomlab 400 dose calibrator (Biodex). 10 µL of each elution fraction was electrophoresed on a 12% SDS-PAGE gel under reducing conditions and evaluated by autoradiography using a BAS-5000 phospho-rimager (Fujifilm). Radiochemical yields and purity were determined by thin layer chromatography on TLC Silica Gel 60 F_{254} (Merck KGaA, Germany) using a 5:1 (v/v) mixture of ethyl acetate: hexane as the eluent. Fractions containing high specific activity fluorobenzoylated scFv-B43.13 ([18F]FBz-scFv-B43.13) were pooled together and used for further *in vitro* and *in vivo* radiopharmacological experiments. The same procedure was also applied for the 18F-labeling of MAb-B43.13, which was used as a positive control for *in vitro* binding and cell uptake studies.

In vitro analysis

Cell uptake studies: OVCAR3 and SKOV3 cells were seeded to obtain $2.5 × 10^5$ cells per well in 12-well tissue culture plates. Complete growth media was removed and cells were rinsed twice with PBS and incubated in Krebs buffer at 37°C for 1 h prior to initiation of the uptake studies. The 18F-labeled MAb-B43.13 and [18F]FBz-scFv-B43.13 (0.1 MBq) were added separately to wells except those assigned to serve as background controls. Cell uptake was terminated at 5, 10, 15, 30, 60, 90, 120 min by adding ice cold Krebs buffer and rinsing the wells twice to wash unbound [18F] FBz-scFv-B43.13 or [18F]FBz-MAb-B43.13 prior to cell lysis with RIPA buffer. The cell lysates were measured for radioactivity on a γ-counter (Wizard²® 2480 Automatic Gamma Counter, Perkin-Elmer, Canada). Protein levels were quantified using a Pierce™ BCA protein assay kit. Cell uptake levels were normalized to percent of the total amount of radioactivity per milligram of protein (% radioactivity/mg protein) and plotted as a function of time. All experiments were performed in triplicates.

Determination of EC_{50} values: Similarly, blocking studies were performed with OVCAR3 cells using two sets of 12-well tissue culture plates containing ~$2.5 × 10^5$ cells per well. One set of 12-well plates was used to evaluate the cell uptake of [18F]FBz-MAb-B43.13 at time points between 5-120 min as described above. In the other set, a competition was allowed to occur by co-incubating 1 mg of unlabeled MAb-B43.13 with 0.1 MBq of 18F-labeled MAb-B43.13 per well and assayed over the same time points as described in the cell uptake experiments. The cell uptake was terminated by the addition of ice-cold Krebs buffer and the cells were processed and measured for the concentration of radioactivity. EC_{50} values were determined via titration of the cell uptake using 0.1 MBq [18F]FBz-MAb-B43.13 or [18F]FBz-scFv-B43.13 with co-incubated concentrations (10^{-5}-10^{-12} M) of unlabeled MAb-B43.13 over a fixed time period of 90 min at 37°C.

Antigen saturation binding assay: The *in vitro* immunoreactivity of [18F]-FBz-scFv-B43.13 for OVCAR3 cells was further confirmed using an antigen saturation-binding assay. To this end, a 0.4 µg/mL solution of [18F]FBz-scFv-B43.13 was prepared in PBS supplemented with 1% BSA.

Twenty microliters of the radioimmunoconjugate solution was added to a microcentrifuge tube containing 10×10^6 cells in 200 μL of culture media. The resulting mixture was incubated for 1 h on ice with intermittent tapping to resuspend the cells. The cells were pelleted via centrifugation (600 × g for 3 min) and the supernatant was pipetted to a separate microcentrifuge tube. The cells were washed with 1 mL of ice-cold PBS and centrifuged (600 × g for 3 min) before pipetting the supernatant to yet another centrifuge tube. This washing procedure was repeated two more times. Finally, the cell pellet, the media supernatant, and the three wash fractions were measured for radioactivity on a gamma counter calibrated for ^{18}F.

The immunoreactive fraction of the radioimmunoconjugate was determined using the formula:

$$Immunoreactive\ Fraction = [Counts_{Cell\ Pellet}]/[Counts_{Cell\ Pellet} + Counts_{Media\ Supernatant} + Counts_{Wash1} + Counts_{Wash2} + Counts_{Wash3}].$$

In vivo experiments

Xenograft models: All experiments were carried out according to guidelines of the Canadian Council on Animal Care (CCAC) and protocol number AC11191 approved by the local animal care committee of the Cross Cancer Institute, Edmonton. Six weeks old NIH-III female mice were obtained from Charles River labs (Quebec, Canada). The animals were housed in ventilated cages and provided food and water *ad libitum*. OVCAR3 tumors were induced on the left shoulder by two subsequent subcutaneous injections of 15×10^6 and 10×10^6 cells in a 300 μL suspension of 1:1 mixture of PBS and matrigel (BD Biosciences). The second injection of cells was administered at the same site within 7-10 days. OVCAR3 tumors grew for 8-10 weeks before reaching tumor sizes of 150-200 mm³. SKOV3 tumors were induced on the left shoulder by a single subcutaneous injection of 5×10^6 cells in PBS and were grown for about 4-5 weeks before they achieved similar tumor sizes.

Small animal PET imaging: Positron emission tomography (PET) experiments were performed separately with OVCAR3 and SKOV3 tumor-bearing NIH-III mice after injecting [^{18}F]FBz-scFv-B43.13. For radiotracer injections, a catheter was placed into the tail vein of the mouse.

Mice were anaesthetized and placed in prone position into the centre of the field of view on a microPET R4 or Inveon PET scanner (Siemens Preclinical Solutions, Knoxville, TN, USA). ~7 MBq of [^{18}F]FBz-B43.13-scFv in 150 μL saline was injected intravenously through the catheter into the tail vein. PET acquisition continued for 60 min in 3D list mode. The dynamic list mode data were sorted into sinograms with 53 time frames (10 × 2, 8 × 5, 6 × 10, 6 × 20, 8 × 60, 10 × 120, 5 × 300 s). The frames were reconstructed using Ordered Subset Expectation Maximization (OSEM) or maximum a posteriori (MAP) reconstruction modes. Correction for partial volume effects was not performed. The image files were further processed using the ROVER v2.0.51 software (ABX GmbH, Radeberg, Germany). Masks defining 3D regions of interest (ROI) were set and the ROIs were defined by thresholding. Mean standardized uptake values [SUV_{mean} = (activity/mL tissue)/(injected activity/body weight), mL/g] were calculated for each ROI. Time-activity curves (TAC) were generated and the semi-quantified PET data are presented as means ± SEM.

Results

Production and characterization of scFv-B43.13

The scFv-B43.13 was purified via immobilized metal affinity chromatography in yields of 1 mg/L of recombinant bacterial culture. Both B43.13 scFv and MAb were fluorescently labeled with two moles of FITC conjugated per mole of the antibody vectors. Immunostaining revealed membrane bound fluorescence in OVCAR3 cells incubated with the CA125 targeting antibody vectors, while no binding was observed in CA125-negative SKOV3 cells (**Figure 2A-D**). Flow cytometry analyses of FITC-MAb-B43.13 and FITC-scFv-B43.13 for binding with CA125 on OVCAR3 cells revealed a shift in forward scatter of fluorescence, which indicated a retained post-labeling immunoreactivity of the CA125 targeting vectors. The control samples showed no shift of forward scatter of fluorescence as seen in the histogram (**Figure 2E**).

[^{18}F]SFB synthesis and radiolabeling of scFv-B43.13

Automated synthesis of *N*-succinimidyl-4-[^{18}F]fluorobenzoate [^{18}F]SFB afforded 67 ± 19%
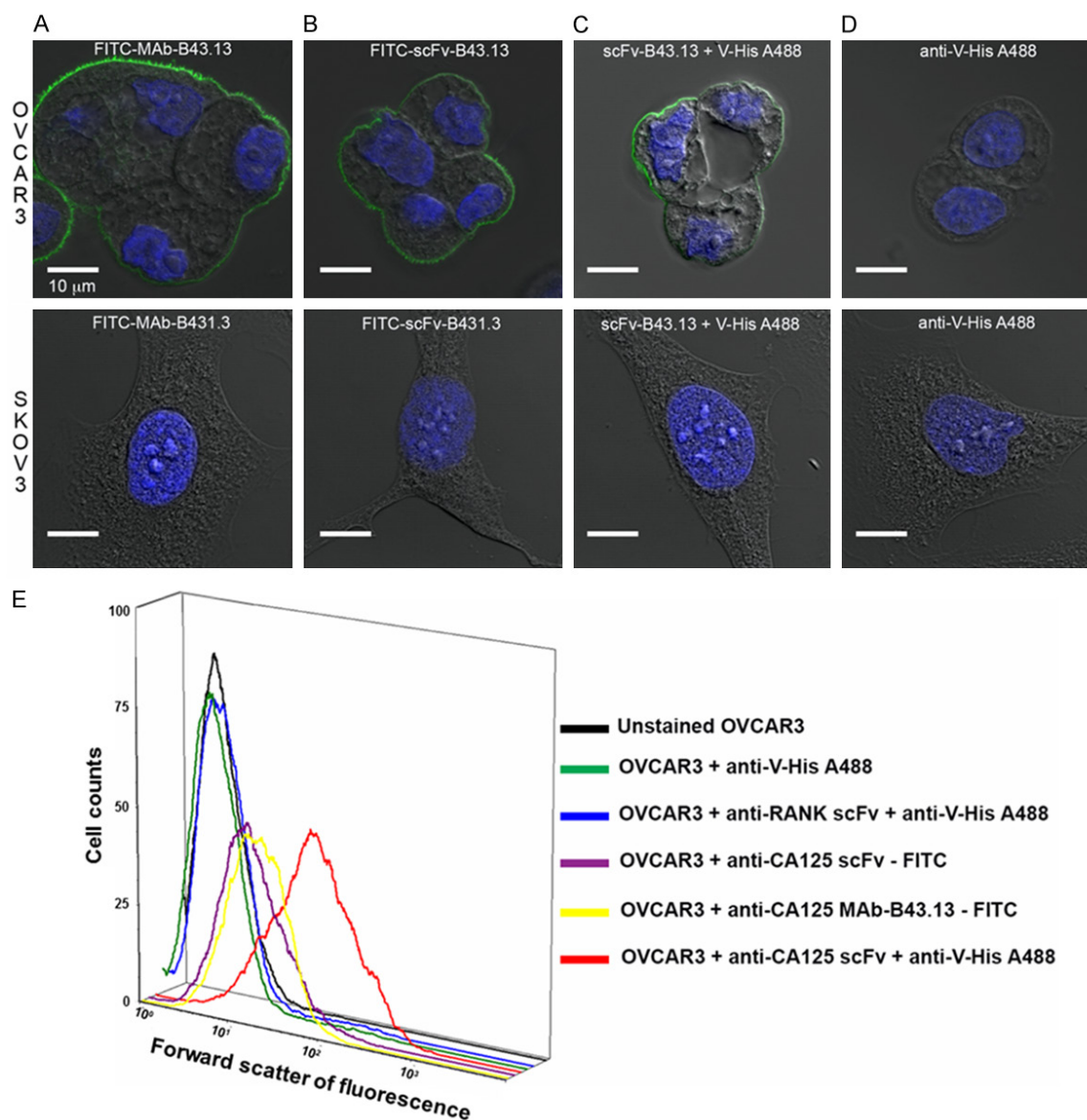
Figure 2. Functional Characterization of B43.13-scFv via Immunostaining and Flow Cytometry Analyses. Confocal images of OVCAR3 cells (top panel) and SKOV3 cells (bottom panel) immunostained with - A. FITC-labeled MAb-B43.13; B. FITC-labeled scFv-B43.13; C. scFv-B43.13; D. Alexa fluor 488-conjugated anti-penta histidine (V-His A488) antibody. The membrane-localized green fluorescence is a typical immunostaining pattern observed for CA125 staining in MUC16-positive cells. E. A three-dimensional histogram representation of the flow cytometry analyses of the scFv-B43.13 and control samples incubated with OVCAR3 cells. The X-axis represents forward scatter of fluorescence and Y-axis represents the cell counts.

radiochemical yield, (decay corrected) over a total synthesis time of 58 ± 4 min with > 95% radiochemical purity (n = 25). The maximum [18F]SFB activity achieved was 9.8 GBq starting from 17.0 GBq of cyclotron-produced [18F]fluoride. 18F-labeled scFv-B43.13 was obtained in radiochemical yields of 3.68 ± 1.81% (n = 5) with a specific activity of 3.88 ± 0.76 GBq/µmol (n = 5). Further purification of [18F]FBz-scFv-B43.13 from non-reacted [18F]SFB and its degradation intermediate 4-[18F]fluorobenzoic acid in borate buffer (pH 8.3) was achieved via size exclusion chromatography on an EconoPac® 10DG desalting column. This afforded [18F]FBz-scFv-B43.13 in >97% purity as analyzed from phosphor-images of the eluted samples electrophoresed on a 12% SDS-polyacrylamide gel (**Figure 3**).

A

B
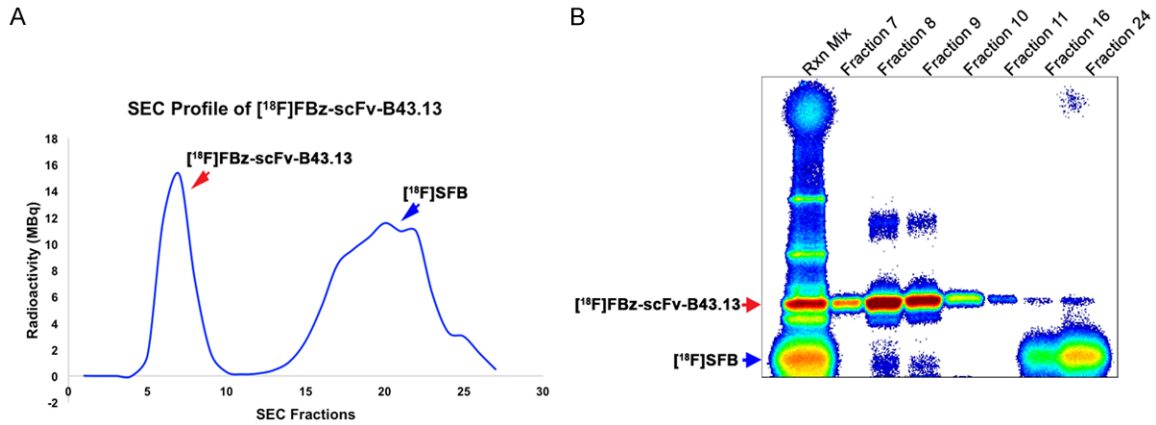
Figure 3. Quality Control Analysis of [^{18}F]FBz-scFv-B43.13. (A) Size exclusion chromatography (SEC) separation profile for the purification of [^{18}F]FBz-scFv-B43.13 from the unreacted and degraded [^{18}F]SFB; (B) Phosphorimage analysis of a SDS-PAGE of the corresponding fractions from the SEC is given in (A). Early SEC fractions (7-10) contained the radiotracer-[^{18}F]FBz-scFv-B43.13, whereas later fractions (15-25) mainly contained unreacted and degraded [^{18}F]SFB.
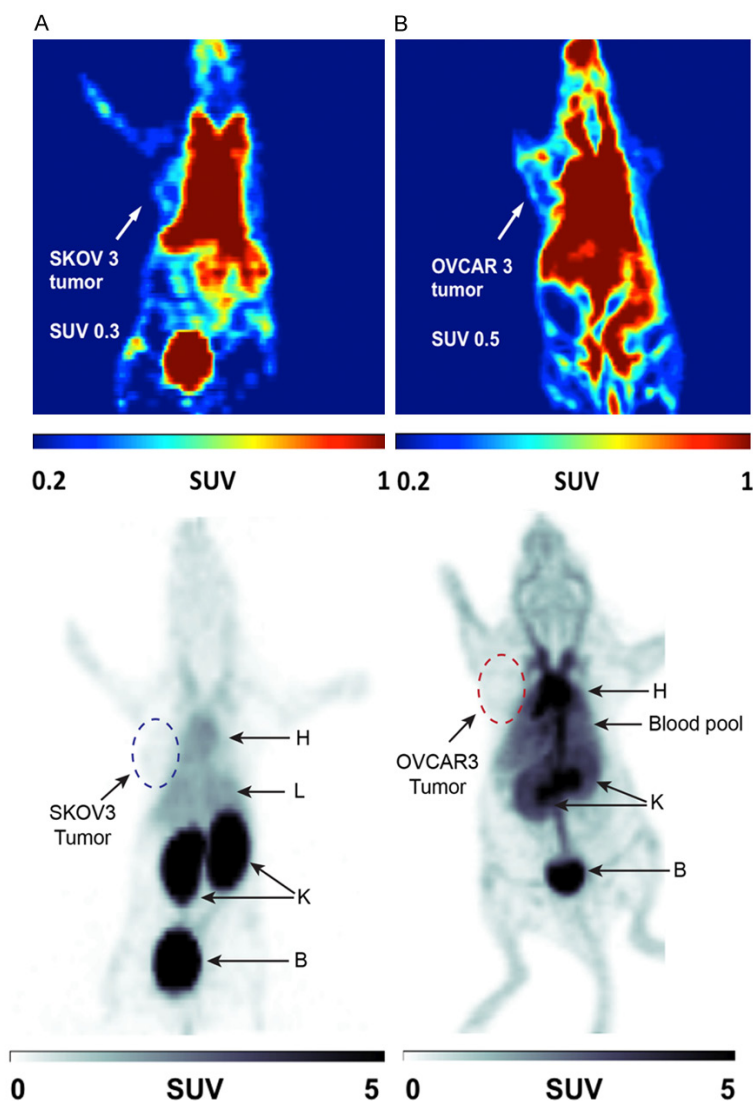
A

B

C
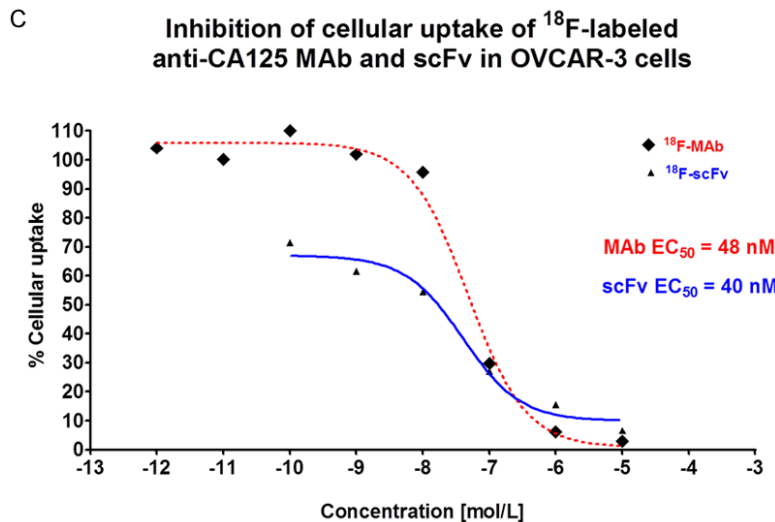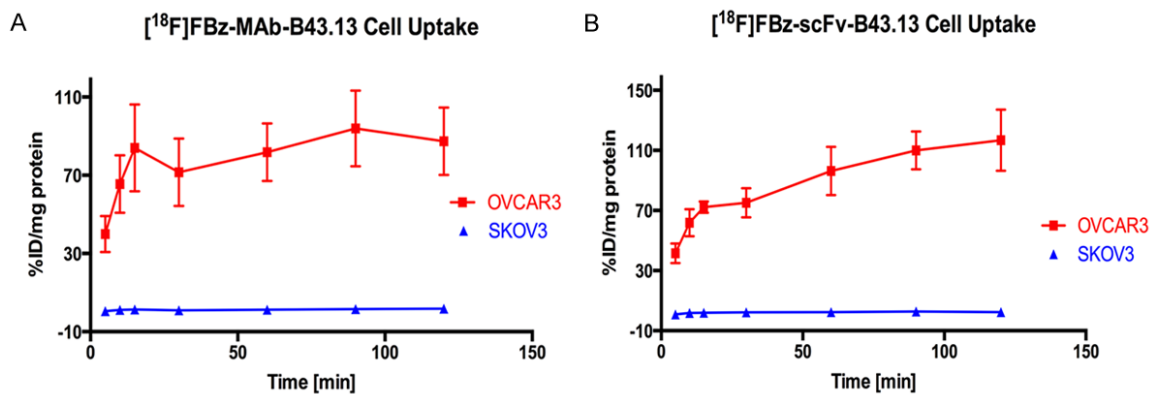
Figure 4. *In vitro* Cell Binding Analyses of [^{18}F]FBz-scFv-B43.13. CA125-positive OVCAR3 versus CA125-negative SKOV3 cells were used to evaluate the binding of (A) [18F]FBz-MAb-B43.13 and (B) [18F]FBz-scFv-B43.13 to the target antigen CA125. (C) A non-linear regression analysis plot of the [^{18}F]FBz-MAb-B43.13 versus [^{18}F]FBz-scFv-B43.13 binding to CA125-positive OVCAR3 cells in the presence of unlabeled MAb-B43.13. EC$_{50}$ values for the binding of the two vectors was calculated using this plot and comparable results were obtained.

In vitro functional characterization of [^{18}F]FBz-scFv-B43.13

SEC-purified [^{18}F]FBz-MAb-B43.13 as well as [^{18}F]FBz-scFv-B43.13 showed specific binding to OVCAR3 and virtually no binding with SKOV3 cells that were used for the *in vitro* cell uptake studies (**Figure 4A** and **4B**). Inhibition studies carried out using ^{18}F-labeled B43.13-MAb and -scFv provided *in vitro* EC$_{50}$ values of 48 nM for

Small animal imaging

In vivo analysis of [^{18}F]FBz-scFv-B43.13 via small animal PET imaging in NIH-III mice bearing OVCAR3 and SKOV3 tumors demonstrated that most of the radioactivity was circulating in the blood pool or concentrated within the organs of clearance such as kidney and liver (**Figure 5**). At 1 h p.i. of [^{18}F]FBz-scFv-B43.13, relatively high amounts of radioactivity were still present in the blood pool of CA125-positive OVCAR3 xenograft mice, while the tumor itself had an SUV$_{mean}$ of 0.5 (n = 3). The CA125-negative SKOV3 tumors had a lower SUV$_{mean}$ of 0.3 (n = 2).

Analysis of time-activity curves derived from the 1 h dynamic PET scans revealed a conformity with the aforementioned observation of considerably higher amounts of [^{18}F]FBz-scFv-B43.13 in the blood pool of OVCAR3-xenograft mice versus SKOV3-xenograft mice injected with the same amount of radiotracer (**Figure 5**). Although [^{18}F]FBz-scFv-B43.13 was expected to be renally cleared (via kidneys and bladder), the radiotracer conformed to this expected renal clearance pathway only in SKOV3-xenograft mice (**Figure 5A**). In contrast, radiotracer [^{18}F]FBz-scFv-B43.13 displayed combination of renal and hepatobiliary elimination pathway in OVCAR3 tumor-bearing mice (**Figure 6B**).

Figure 5. *In vivo* Small Animal PET Imaging Analysis. Representative PET images of NIH-III mice subcutaneously xenografted with (A) SKOV3 (CA125-negative) tumors and (B) OVCAR3 (CA125-positive) tumors on the left shoulder. The mice were intravenously injected with ~7 MBq of [^{18}F]FBz-B43.13-scFv in 150 μL saline through the tail vein and dynamic PET imaging was performed for 1 h. The top panel shows coloured coronal planar slices scaled from SUV = 0.2 to 1.0 to delineate the tumor margins, whereas the lower panel shows a grayscale coronal slice of the same image scaled from SUV = 0 to 5 to highlight the differences of the distribution and clearance profile of the radiotracer between the two tumor xenograft models. At 1 h p.i., radiotracer [^{18}F]FBz-B43.13-scFv accumulated more in kidneys (K) and bladder (B) of SKOV3-xenograft mice whereas it lingered longer in the blood pool (heart-H and liver-L) of OVCAR3-xenograft mice.

the [^{18}F]FBz-MAb-B43.13 and 40 nM for the [^{18}F]FBz-scFv-B43.13. These values were comparable for both the radiotracers co-incubated with unlabeled MAb-B43.13 (**Figure 4C**). However, saturation binding studies with [^{18}F]FBz-scFv-B43.13 and OVCAR3 cells indicated that only 51% of the prepared radiotracer fraction was immunoreactive.

Discussion

Immuno-PET relies on the ability of antibody-based targeting vectors to specifically bind with the target antigen *in vivo*. Since antibody fragments described in this work are mostly produced via recombinant methods, it is vital that they are prepared in high purity and retain their
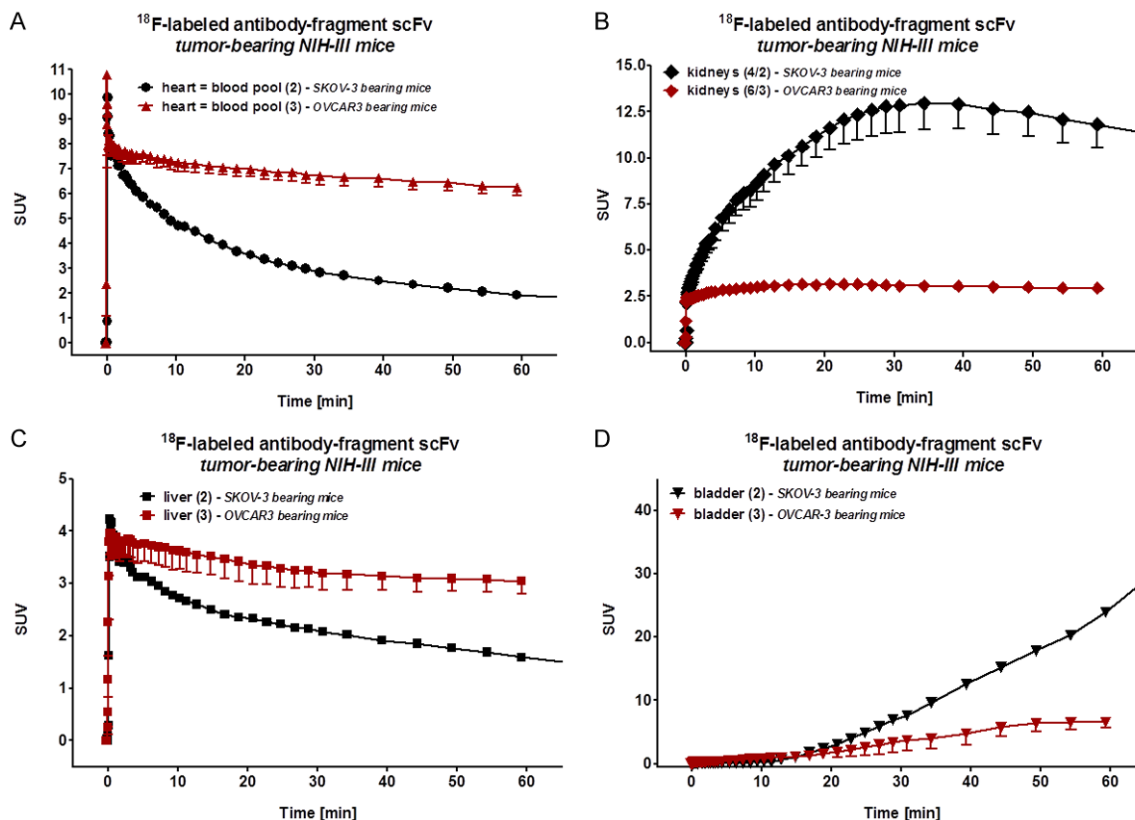
Figure 6. *In vivo* Time Activity Curves of the Radiotracer. Analysis of the time activity curves (TAC) from 1 h dynamic PET scans of [18F]FBz-B43.13-scFv in the various tissue compartments of OVCAR3 versus SKOV3 tumor bearing NIH-III mice - A. Blood pool-heart; B. Liver; C. Kidneys; D. Bladder. A significantly higher amount of the radiotracer remained in the blood pool and followed a hepatobiliary clearance pathway in the OVCAR3 xenografts, whereas rapid renal clearance pattern was dominant in SKOV3 xenografts.

biochemical affinity for binding to the target antigen [16]. In the present work, this was achieved via expression and folding of the targeting vector B43.13 scFv within an oxidizing environment of the periplasm of recombinant *E.coli*, and its subsequent purification via immobilized metal affinity chromatography. As a preliminary assessment of functional activity, CA125-targeting scFv and MAb were conjugated with FITC using fluorescein isothiocyanate owing to the latter's ability for stable thiourea bond formation with primary amines within biomolecules under slightly basic pH conditions. Our observation of membrane-localized fluorescence confirmed successful binding of the FITC-MAb-B43.13 and FITC-scFv-B43.13 immuno-conjugates to CA125 in CA125-positive OVCAR3 cells. This was in agreement with previously reported FITC-labeled CA125-targeting antibodies-MAb-B43.13 and MAb-B27.1 [17].

After successful demonstration of specific binding of fluorescently labeled targeting vectors-MAb-B43.13 and scFv-B43.13 to CA125 *in vitro*, we performed radiolabeling of the scFv-B43.13 with 18F to develop a molecular probe that could be used for immuno-PET imaging of EOC. Direct radiofluorination procedures often use harsh conditions that could potentially destroy the structure and function of delicate biomolecules such as antibody fragments. Therefore we selected the prosthetic group *N*-succinimidyl-4-[18F]fluorobenzoate ([18F]SFB) to perform a bioconjugation reaction under mild conditions compatible with the structural and functional integrity of immunoconjugates [18]. In accordance with previous reports and our own experience, we purified [18F]SFB via HPLC to obtain high purity [18F]SFB to achieve higher coupling yields and to preserve the immunoreactivity of the antibody fragment [19, 20]. As an an active ester, [18F]SFB reacts rap-

idly via acylation reaction with primary amines present within biomolecules such as scFv-B43.13 and forms stable amide bonds that ultimately yield an ^{18}F-fluorobenzoylated version of the targeting agent-[^{18}F]FBz-scFvB43.13. However, we observed that the efficiency of radio-fluorination using [^{18}F]SFB was impacted by partly degradation of the prosthetic group under basic conditions that are required for the proposed acylation reaction with primary amines like lysine residues. Moreover, acylation reaction with [^{18}F]SFB proceeded randomly at primary amine groups present in the antibody fragment.

Random labeling of scFv-B43.13 with [^{18}F]SFB resulted in the formation of a radiolabeled immunoconjugate with reduced immunoreactivity. However, despite the moderate 51% immunoreactivity of [^{18}F]FBz-scFv-B43.13, the radiotracer demonstrated specific binding to OVCAR3 cells in cell uptake studies and yielded an EC_{50} value comparable to that of the parent full-length antibody-MAb-B43.13. Other ^{18}F-labeled scFv(s) with similar immunoreactivity have previously been demonstrated to visualize tumors *in vivo* [21, 22]. Recent work on novel innovative approaches for the preparation of site-specifically labeled immunoconjugates for molecular imaging purposes may open new directions for a more defined bioconjugation of radiolabels and other reporters to delicate proteins like antibodies and antibody fragments to preserve structural and functional integrity of the labeled immunoconjugates for high immunoreactivity [23, 24].

Our previous studies with the scFv-B43.13 revealed that it had similar off-rate kinetics as its parent antibody-MAb-B43.13. However, under the effect of first pass clearance, the *in vivo* accretion of the ^{64}Cu-labeled scFv-B43.13 (^{64}Cu-NOTA-scFv-B43.13) did not improve significantly beyond 1 h p.i., even though the amount of circulating radiotracer had decreased at 24 h p.i. [25]. A combination of our previous experience in working with ^{64}Cu-NOTA-scFv-B43.13 and the present *in vitro* results motivated us to synthesize and test [^{18}F]FBz-scFv-B43.13 as a CA125 targeting vector for *in vivo* application at early time points.

Due to the obvious fact that the radiopharmacological profile of the full-length *in vivo* antibody [^{18}F]FBz-MAb-B43.13 would not meet the requirements of a same day PET imaging protocol, only [^{18}F]FBz-scFv-B43.13 was used in our described PET imaging experiments. PET imaging of the radiolabeled immunoconjugate at 1 h p.i. revealed higher radioactivity levels in the blood in OVCAR3 tumor-bearing mice compared to SKOV3 tumor bearing mice. PET images in **Figure 5** reflect a limited bioavailability of the radiotracer at the tumor site resulting in difficulties of a clear delineation of the CA125-positve tumors. However, time-activity curves derived from the 1 h dynamic PET scans revealed higher tumor-to-muscle ratio in OVCAR3 tumor bearing mice compared to SKOV3 tumors. Furthermore, PET imaging in OVCAR3 tumor-bearing mice showed that the radiotracer [^{18}F]FBz-scFv-B43.13 follows a combined renal and hepatobiliarly elimination pathway. This finding is in contrast to the expected dominant renal clearance profile that is typically observed for scFv-based and other radiotracers with molecular weights below 60 kDa.

This finding may be attributed to the potential formation of immunocomplexes between the tracer quantities of [^{18}F]FBz-scFv-B43.13 and any shed CA125 antigen that may be present within the bloodstream of mice xenografted with OVCAR3 tumors. However, several attempts to quantify *in vivo* shed CA125 antigen via immunoassays using serum from subcutaneously xenografted OVCAR3 mice models did not yield any detectable titers for the antigen whatsoever. Nevertheless, immunocomplex formation of ^{99m}Tc-MAb-B43.13 with shed CA125 antigen within the first 90 min after injection of the radiotracer and subsequent clearance via the liver was reported by McQuarrie et al. in ovarian cancer patients undergoing radioimmunoscintigraphy. In their studies a relatively high imaging dose of 2 mg of ^{99m}Tc-MAb-B43.13 injected per patient maintained the bioavailability of the radiotracer despite immune-complex formation and clearance [26, 27]. Another possible explanation is the low immunoreactivity (51%) and the reduced functional affinity (avidity) of the radiolabeled antibody fragment [^{18}F]FBz-scFv-B43.13 compared to the full antibody.

In summary, despite the promising *in vitro* target binding capabilities, the use of scFv(s) as ideal targeting vectors is greatly limited by their molecular weight/size. Paradoxically, the latter
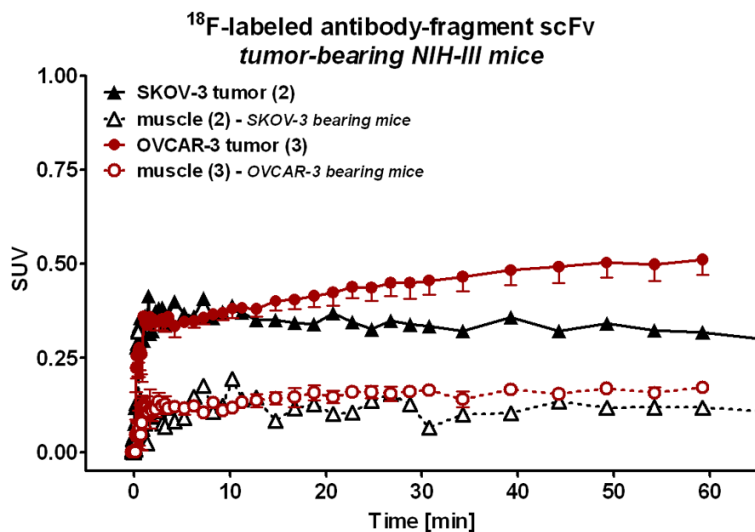
Figure 7. Tumor and Muscle Uptake of the Radiotracer. Time-activity curves of the tumor and muscle uptake of [18F]FBz-B43.13-scFv over time revealed similar muscle uptake profile of the radiotracer in SKOV3 and OVCAR3-tumor bearing mice, whereas radiotracer uptake was higher in CA125-positive OVCAR3 tumors compared to CA125-negative SKOV3 tumors.

was proposed to be a prime advantage for using the scFv format to achieve high contrast images within shorter periods of time post-injection of the radiotracer. However, other reports have also demonstrated that monomeric scFv(s) becomes a victim of first pass clearance and get trapped within the renal system [21, 22, 28]. An evaluation by Wittrup *et al.* to identify the ideal size of tumor targeting agents described scFv molecules as residing in the death-valley of the curve [29]. This analogy is supported by the explanation that scFv(s) are too small to escape renal clearance and too big for rapid extravasation from blood vessels that carry them to the tumor. Further, a lack of sufficient avidity combined with a potentially compromised affinity due to radiofluorination that may be occurring at lysines within the target binding pockets of the scFv may also contribute to a loss of *in vivo* binding efficacy of the scFv. Therefore, diabodies with engineered cysteines that facilitate site-specific labeling have been proposed to yield relatively better *in vivo* tumor uptake of antibody fragments [30, 31].

Finally, the presence of a polar hexa-histidine tag at the C-terminus of the scFv and the overall positive charge of this molecule (attributed to the amino acid composition of the scFv) may be additional factors that contribute to its

absorption and retention within the proximal tubules of kidneys [32, 33].

Pre-dosing with positively charged amino acids like poly-L-lysine (1.2 g/kg) has been used for peptide-receptor radionuclide therapy (PRRT). Co-infusion of succinylated gelatin (150 mg/kg) was also reported for preclinical immuno-PET applications using nanobodies to circumvent the excessive renal trapping of the radiotracer while concomitantly improving its tumor bioavailability [33]. Finally, in the limited number of animals examined in this study, similar tumor-to-muscle ratios of the radiotracer were observed in both the tumor-bearing xenograft mice, however, there was a slightly higher absolute uptake value of [18F]FBz-scFv-B43.13 in OVCAR3 (CA125-positive) over SKOV3 (CA125-negative) tumors (**Figure 7**).

Clearly, this study warrants further engineering of the scFv-B43.13 as a diabody to improve its avidity and yield better tumor uptake while concomitantly removing the polar hexa-histidine tag to achieve favourable *in vivo* radiopharmacological profiles for same-day PET imaging. Nevertheless, the scFv-B43.13 can be employed as an economically viable analytical reagent in place of MAB-B431.3 for the *in vitro* and *ex vivo* analysis of samples being investigated for the presence of CA125.

Conclusion

A single chain variable fragment (scFv) derived from antibody MAb-B43.13 was produced by recombinant methods and purified as a biochemically active protein capable of binding to CA125 as the target antigen. The antibody fragment was radiofluorinated using [18F]SFB as a prosthetic group to afford radiotracer [18F]FBz-anti-CA125 scFv. PET imaging of [18F]FBz-scFv-B43.13 in preclinical ovarian cancer xenograft mice models revealed a modest tumor uptake in CA125-positive OVCAR3 tumors, which was higher compared to CA125-negative

SKOV3 tumors. However, radiotracer [^{18}F]FBz-scFv-B43.13 demonstrated a remarkably different *in vivo* biodistribution and radiopharmacological profile in both preclinical ovarian cancer models. The present work describes the development and characterization of a CA125-targeted antibody-fragment intended for a same-day immuno-PET imaging procedure of epithelial ovarian cancer. Notably, the present study adds important experimental data to the discussion on potential strengths and limitations of using antibody fragments such as scFv(s) to target and image tumors at early time points in a setting that is challenged further by the presence of shed antigen.

Acknowledgements

Address correspondence to: Frank R Wuest, Department of Oncology, University of Alberta, 11560 University Avenue, Edmonton, AB, T6G 1Z2, Canada. Tel: 780-989-8150; Fax: 780-432-8483; E-mail: wuest@ualberta.ca

References

[1] Knowles SM and Wu AM. Advances in immuno-positron emission tomography: antibodies for molecular imaging in oncology. J Clin Oncol 2012; 30: 3884-3892.

[2] Wu AM. Engineered antibodies for molecular imaging of cancer. Methods 2014; 65: 139-147.

[3] Holliger P and Hudson PJ. Engineered antibody fragments and the rise of single domains. Nat Biotechnol 2005; 23: 1126-1136.

[4] Wu AM and Yazaki PJ. Designer genes: recombinant antibody fragments for biological imaging. Q J Nucl Med 2000; 44: 268-283.

[5] Wu AM. Antibodies and antimatter: the resurgence of immuno-PET. J Nucl Med 2009; 50: 2-5.

[6] Wu AM and Olafsen T. Antibodies for molecular imaging of cancer. Cancer J 2008; 14: 191-197.

[7] Davis HM, Zurawski VR Jr, Bast RC Jr and Klug TL. Characterization of the CA 125 antigen associated with human epithelial ovarian carcinomas. Cancer Res 1986; 46: 6143-6148.

[8] Scholler N and Urban N. CA125 in ovarian cancer. Biomark Med 2007; 1: 513-523.

[9] Capstick V, Maclean GD, Suresh MR, Bodnar D, Lloyd S, Shepert L, Longenecker BM and Krantz M. Clinical evaluation of a new two-site assay for CA125 antigen. Int J Biol Markers 1991; 6: 129-135.

[10] Nustad K, Bast RC Jr, Brien TJ, Nilsson O, Seguin P, Suresh MR, Saga T, Nozawa S, Bormer OP, de Bruijn HW, Nap M, Vitali A, Gadnell M, Clark J, Shigemasa K, Karlsson B, Kreutz FT, Jette D, Sakahara H, Endo K, Paus E, Warren D, Hammarstrom S, Kenemans P and Hilgers J. Specificity and affinity of 26 monoclonal antibodies against the CA 125 antigen: first report from the ISOBM TD-1 workshop. International Society for Oncodevelopmental Biology and Medicine. Tumour Biol 1996; 17: 196-219.

[11] Nap M, Vitali A, Nustad K, Bast RC Jr, O'Brien TJ, Nilsson O, Seguin P, Suresh MR, Bormer OP, Saga T, de Bruijn HW, Nozawa S, Kreutz FT, Jette D, Sakahara H, Gadnell M, Endo K, Barlow EH, Warren D, Paus E, Hammarstrom S, Kenemans P and Hilgers J. Immunohistochemical characterization of 22 monoclonal antibodies against the CA125 antigen: 2nd report from the ISOBM TD-1 Workshop. Tumour Biol 1996; 17: 325-331.

[12] Berek JS. Immunotherapy of ovarian cancer with antibodies: a focus on oregovomab. Expert Opin Biol Ther 2004; 4: 1159-1165.

[13] Iagaru AH, Mittra ES, McDougall IR, Quon A and Gambhir SS. 18F-FDG PET/CT evaluation of patients with ovarian carcinoma. Nucl Med Commun 2008; 29: 1046-1051.

[14] Sharma SK, Suresh MR and Wuest FR. Improved soluble expression of a single-chain antibody fragment in E. coli for targeting CA125 in epithelial ovarian cancer. Protein Expr Purif 2014; 102: 27-37.

[15] Mading P, Fuchtner F and Wust F. Module-assisted synthesis of the bifunctional labelling agent N-succinimidyl 4-[(18)F]fluorobenzoate ([(18)F]SFB). Appl Radiat Isot 2005; 63: 329-332.

[16] Olafsen T and Wu AM. Antibody vectors for imaging. Semin Nucl Med 2010; 40: 167-181.

[17] Xiao Z, McQuarrie SA, Suresh MR, Mercer JR, Gupta S and Miller GG. A three-step strategy for targeting drug carriers to human ovarian carcinoma cells in vitro. J Biotechnol 2002; 94: 171-184.

[18] Wester HJ, Hamacher K and Stocklin G. A comparative study of N.C.A. fluorine-18 labeling of proteins via acylation and photochemical conjugation. Nucl Med Biol 1996; 23: 365-372.

[19] Vaidyanathan G and Zalutsky MR. Improved synthesis of N-succinimidyl 4-[18F]fluorobenzoate and its application to the labeling of a monoclonal antibody fragment. Bioconjug Chem 1994; 5: 352-356.

[20] Garg PK, Garg S and Zalutsky MR. Fluorine-18 labeling of monoclonal antibodies and fragments with preservation of immunoreactivity. Bioconjug Chem 1991; 2: 44-49.

[21] Cai W, Olafsen T, Zhang X, Cao Q, Gambhir SS, Williams LE, Wu AM and Chen X. PET imaging of colorectal cancer in xenograft-bearing mice by use of an 18F-labeled T84.66 anti-carcino-embryonic antigen diabody. J Nucl Med 2007; 48: 304-310.

[22] Olafsen T, Sirk SJ, Olma S, Shen CK and Wu AM. ImmunoPET using engineered antibody fragments: fluorine-18 labeled diabodies for same-day imaging. Tumour Biol 2012; 33: 669-677.

[23] Adumeau P, Sharma SK, Brent C, Zeglis BM. Site-Specifically Labeled Immunoconjugates for Molecular Imaging-Part 2: Peptide Tags and Unnatural Amino Acids. Mol Imaging Biol 2016; 18: 153-65.

[24] Adumeau P, Sharma SK, Brent C, Zeglis BM. Site-Specifically Labeled Immunoconjugates for Molecular Imaging--Part 1: Cysteine Residues and Glycans. Mol Imaging Biol 2016; 18: 1-17.

[25] Sharma SK, Wuest M, Wang M, Glubrecht D, Andrais B, Lapi SE and Wuest F. Immuno-PET of epithelial ovarian cancer: harnessing the potential of CA125 for non-invasive imaging. EJNMMI Res 2014; 4: 60.

[26] McQuarrie SA, Riauka T, Baum RP, Sykes TR, Noujaim AA, Boniface G, MacLean GD and McEwan AJ. The effects of circulating antigen on the pharmacokinetics and radioimmunoscintigraphic properties of 99m Tc labelled monoclonal antibodies in cancer patients. J Pharm Pharm Sci 1998; 1: 115-125.

[27] McQuarrie SA, Baum RP, Niesen A, Madiyalakan R, Korz W, Sykes TR, Sykes CJ, Hor G, McEwan AJ and Noujaim AA. Pharmacokinetics and radiation dosimetry of 99Tcm-labelled monoclonal antibody B43.13 in ovarian cancer patients. Nucl Med Commun 1997; 18: 878-886.

[28] Williams LE, Wu AM, Yazaki PJ, Liu A, Raubitschek AA, Shively JE and Wong JY. Numerical selection of optimal tumor imaging agents with application to engineered antibodies. Cancer Biother Radiopharm 2001; 16: 25-35.

[29] Wittrup KD, Thurber GM, Schmidt MM and Rhoden JJ. Practical theoretic guidance for the design of tumor-targeting agents. Methods Enzymol 2012; 503: 255-268.

[30] Schneider DW, Heitner T, Alicke B, Light DR, McLean K, Satozawa N, Parry G, Yoo J, Lewis JS and Parry R. In vivo biodistribution, PET imaging, and tumor accumulation of 86Y- and 111In-antimindin/RG-1, engineered antibody fragments in LNCaP tumor-bearing nude mice. J Nucl Med 2009; 50: 435-443.

[31] Eder M, Knackmuss S, Le Gall F, Reusch U, Rybin V, Little M, Haberkorn U, Mier W and Eisenhut M. 68Ga-labelled recombinant antibody variants for immuno-PET imaging of solid tumours. Eur J Nucl Med Mol Imaging 2010; 37: 1397-1407.

[32] Vegt E, de Jong M, Wetzels JF, Masereeuw R, Melis M, Oyen WJ, Gotthardt M and Boerman OC. Renal toxicity of radiolabeled peptides and antibody fragments: mechanisms, impact on radionuclide therapy, and strategies for prevention. J Nucl Med 2010; 51: 1049-1058.

[33] D'Huyvetter M, Vincke C, Xavier C, Aerts A, Impens N, Baatout S, De Raeve H, Muyldermans S, Caveliers V, Devoogdt N and Lahoutte T. Targeted radionuclide therapy with A 177Lu-labeled anti-HER2 nanobody. Theranostics 2014; 4: 708-720.